2. MEASUREMENT SYSTEM DESCRIPTION

The mobile noise measurement system (NMS) consists of a computer, receiver, antenna, and vehicle. This section describes the design and operation of the NMS.

2.1 Vehicle

Noise measurements were conducted at many sites over a wide geographic range in the Denver metropolitan area. For convenience, all measurements were obtained with the NMS installed in a vehicle. The vehicle is an extended-length van powered by a diesel engine. An aluminum sheet was welded to the top of the van to serve as a ground plane for the antenna. Instrument racks were installed in the rear of the van to hold measurement equipment.

2.1.1 Vehicle Power Sources

The power to the instruments was supplied directly from a 120-V ac connection or indirectly by a power inverter. The power inverter produced 120-V ac from the van 12-V dc power system (diesel engine, alternator, voltage regulator, and batteries).

The ac connection was preferred over the power inverter for two reasons. First, the ac connection could provide continuous power for extended measurement periods while the measurements made using the power inverter were limited in time by the size of the van fuel tank. The power inverter also added a small amount of radiated radio frequency interference (RFI) to the measurement results.

2.2 Antenna

Man-made noise is expected to arrive at the horizon from widely scattered directions. The effect of the directional gain on noise power measurements has been of concern [3,8] and has led to suggestions that there should be a standard measurement antenna. The standard most often suggested is a simple, short monopole antenna. This is a good choice at frequencies less than 30 MHz; however, at higher frequencies a more effecient quarter-wave monopole is a better choice.

The quarter-wave monopole antenna used for these measurements was mounted on a rectangular aluminum ground plane attached to the roof of the measurement van. The ground plane dimensions are 3.6m by 1.6m, or 1.648 by 0.738 at 137MHz where 8 is the 2.19 m wavelength.

The quarter-wave monopole antenna pattern is dependant upon the size and shape of the ground plane [9]. A quarter-wave monopole antenna mounted on this ground plane will not have a perfectly omnidirectional antenna pattern; however, the distorted azimuth antenna pattern is not expected to significantly impact measurements. Of more concern was the elevation antenna pattern.

Finite-difference time-domain techniques were used to estimate the elevation antenna pattern. Figure 2.1 depicts the elevation antenna pattern for a quarter-wave monopole antenna mounted on a circular ground plane for three different radii representing the ground plane width (ka = 2.3), length (ka = 5.2), and a point in between (ka = 3.7), where a is the radius and k is *2B/8*. The gain is approximately unity at the horizon for all cases; hence the ground plane size and shape is not expected to significantly impact the measurements.

Like the antenna pattern, the impedance of the quarter-wave monopole antenna depends on the size and shape of the ground plane. The mounted antenna voltage standing-wave ratio is 1.2 with a corresponding transmission loss of 0.04 dB. This measurement shows the impedance of the mounted antenna is well matched to the receiver input impedance.

2.3 Receiver

A custom receiver was built to ensure that wideband noise would not saturate receiver components and interference from other services would be minimized. The receiver has a noise figure of 2.9 dB and a center frequency of 137.0 MHz. The receiver could be tuned over the entire 136.0 to 138.0 MHz VHF meteorological satellite band.

The single conversion superheterodyne design is composed of rf, IF, and video detection stages. Figure 2.2 shows all components used in the receiver construction. Appendix A lists specifications of the components.

2.3.1 The rf Stage

A three-pole Chebyshev preselection filter, F1, with a 4.1-MHz, 3-dB bandwidth rejects the image frequency and strong out-of-band interferers prior to preamplification. A low-noise, high-gain preamplifier, A1, establishes receiver sensitivity. After preamplification, a five-pole Chebyshev image-stripping filter, F2, attenuates noise at the image frequency.

A double balanced mixer driven by a frequency synthesized local oscillator (LO) signal downconverts the signal to a 10.7 MHz IF. A double balanced mixer with a high 1-dB compression point minimizes the introduction of nonlinear effects. The frequency synthesizer has excellent frequency stability and low phase noise.

2.3.2 IF Stage

A low-pass filter (LPF), F3, with a 70-MHz 3-dB cutoff frequency rejects undesirable mixer products that may overload the first IF amplifier. A 10-dB pad, at the input of F3, ensures that reflected signals are attenuated.

The first IF amplifier, A2, boosts the signal before the first IF bandlimiting filter. The first IF filter, F4, has a three-pole Chebyshev response and a 214-kHz 3-dB bandwidth. Reducing the bandwidth from 4.1 MHz to 214 kHz reduces noise power and adjacent channel interference prior to further IF amplification. The 10-dB pad before this filter ensures that reflected signals are attenuated.

The next two amplifiers, A3 and A4, and 6-dB pad, P3, were used to adjust IF gain to correspond to the dynamic range of the log amplifier. The receiver IF gain was designed to measure 16 dB below and 64 dB above the average receiver input noise power.

The final IF bandlimiting filter, F5, is a six-pole Chebyshev crystal filter with a 32-kHz 3-dB bandwidth. This filter was chosen so that all noise measured would be within the APT satellite frequency allocation [10]. The filter noise equivalent bandwidth is approximately 34 kHz. The 10-dB pad, P4, before this filter ensures that reflected signals are attenuated.

2.3.3 Video Detection Stage

A log amplifier (LA) with a dynamic range of 80 dB was used for detection. The log amplifier has a rise and fall time of 700 ns and a 3-dB bandwidth of approximately 6 MHz. The maximum input signal is 0 dBm and the minimum input is -80 dBm. The maximum signal generates 2.2 V and the minimum signal generates 0.1 V. The slope of the log amplifier is 26.25 mV/dB. The log amplifier output is dc coupled so that a continuous wave signal can be used for power calibration.

2.4 Data Acquisition

An industrial computer housed in a metal, shielded case was used for data acquisition. The processor and bus speeds were 133 MHz and 66 MHz, respectively. The computer digitized, stored, and displayed noise power samples and their statistics.

2.4.1 Digitization

The output of the log amplifier was connected to the computer analog-to-digital conversion (ADC) card. The ADC card sampled the voltage at the log amplifier output 1000 times a second. The ADC card has 12 bits that cover 0-10 volts or 2.442 mV/ADC unit. The log amplifier slope is 26.25 mV/dB therefore our amplitude precision was approximately 0.1 dB.

2.4.2 Noise Histograms

Saving every noise power sample would have required tremendous amounts of computer data storage. To alleviate this problem, noise power samples were stored in 1000 histogram bins. The bins had a resolution of 0.1 dB and a range that extended from 26 dB below to 74 dB above the average receiver input noise floor. Each noise histogram contained 60,000 noise power samples that required approximately 60 seconds to digitize, and 50 seconds to develop into a histogram, record, and display on the screen.

2.4.3 Graphical User Interface

As the data were collected, two graphs were visible to the user. The first graph showed the recently acquired noise power samples while the second graph showed the last complete noise histogram.

2.5 Radio Frequency Interference

2.5.1 Radiated Radio Frequency Interference from Out-of-Band Interferers

The superheterodyne receiver may give erroneous results because of intermodulation products from strong out-of-band interferers or failure to properly attenuate image frequency signals. These possibilities were minimized by the proper selection of rf and IF filters and amplifiers. A spectrum survey conducted by ITS was examined to determine out-of-band attenuation requirements [11]. Out-of-band interferer- and image-rejection was measured with a continuous wave signal injected into the receiver input.

2.5.2 Radiated Radio Frequency Interference from NMS

Radiated radio frequency interference (RFI) was found to originate from the computer and power inverter. To suppress this RFI, Type 43 ferrites were placed on all cables coming out of their metal cases and van doors were closed during measurements. Radiated RFI was measured with an antenna in a radio-quiet canyon with the computer and power inverter turned on.

2.5.3 Conducted Radio Frequency Interference

Conducted RFI originating from the ac connection or power inverter was attenuated by power line filtering. Conducted RFI was measured by replacing the antenna with a 50-ohm termination. Conducted RFI was never observed in any of these measurements.

2.6 Verification

The NMS operation was verified with the following measurements: noise power measured with 50 ohm receiver input termination, noise power measured with antenna in a radio-quiet canyon, and continuous wave interference power measured with a continuous wave signal injected at the receiver input.

Figure 2.3 shows median, mean, and peak powers measured with a 50-ohm receiver input termination over a 24-hour period. This measurement was performed to assure measurement repeatability over changing temperatures. Figure 2.4 shows an APD during this extended measurement. This APD indicates that receiver noise is Gaussian.

Figure 2.5 shows an APD obtained with the antenna in a radio-quiet canyon. The van is operating with its power inverter. The mean of this measurement is less than 1 dB higher than the mean with the 50-ohm load.

Figure 2.6 shows an APD obtained with a signal generator connected to the receiver input. The signal generator injected a continuous wave signal with 10 dB more power than the receiver average noise power. The measured APD corresponds to the APD of a Nakagami-Rice distribution with a K factor of approximately 10 dB as expected.

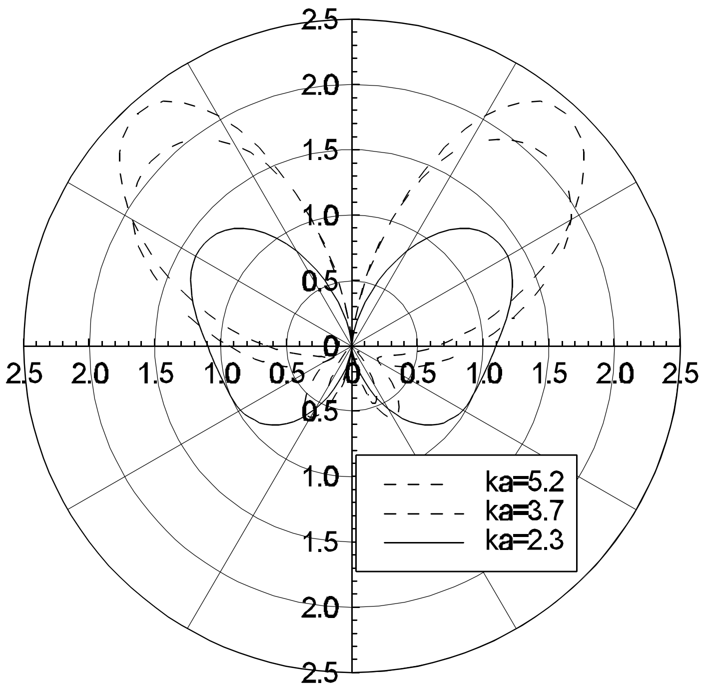

Figure 2.1 Antenna pattern of a quarter-wave monopole antenna over a circular ground plane.

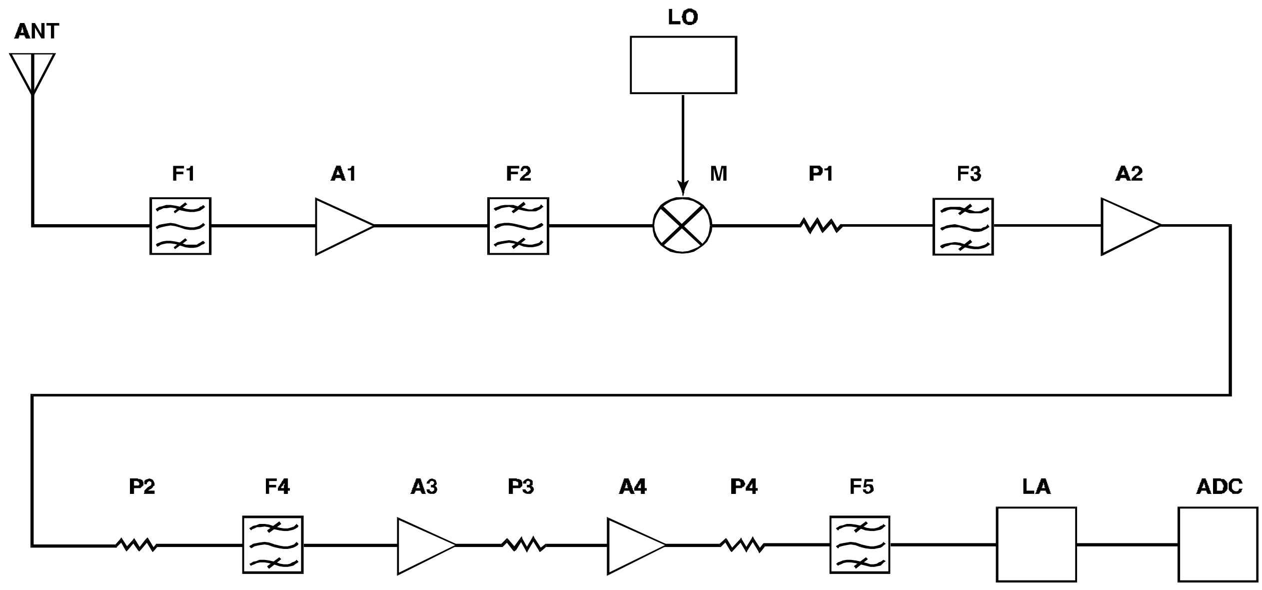

Figure 2.2 Receiver block diagram.

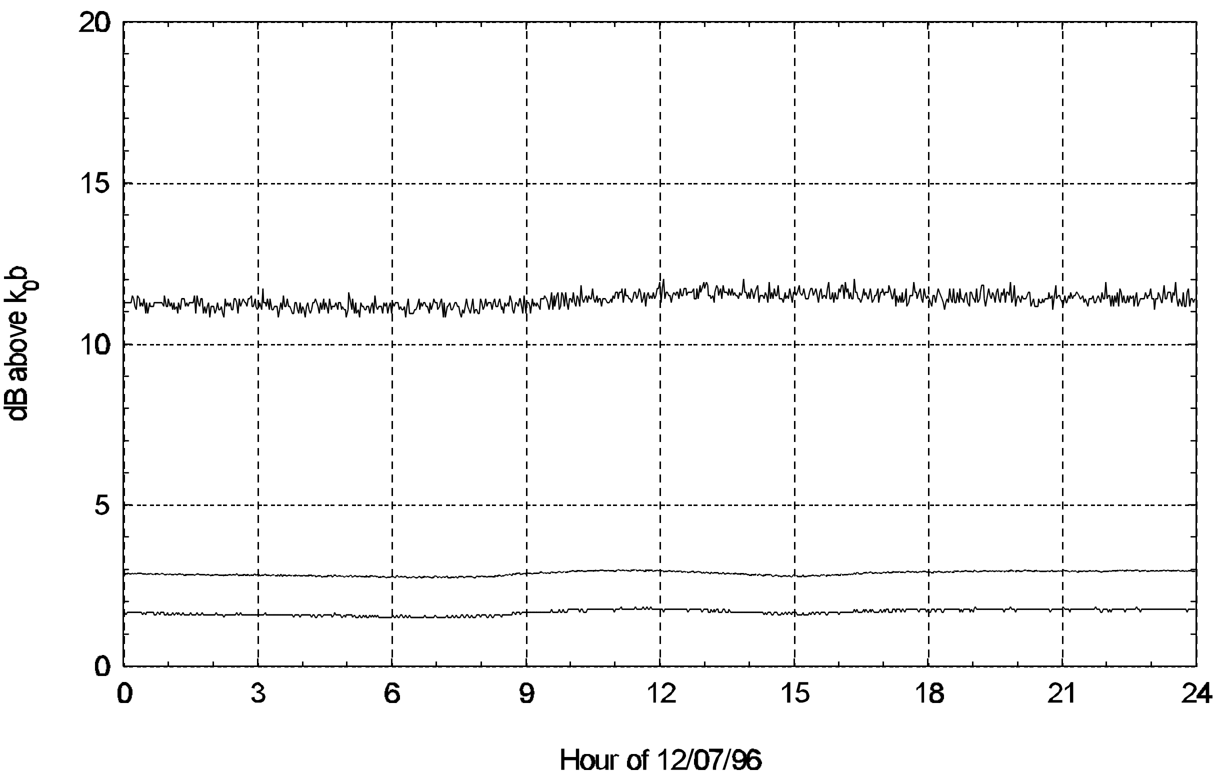

Figure 2.3 Median (bottom), mean (middle), and peak (top) receiver noise power over a 24-h period.

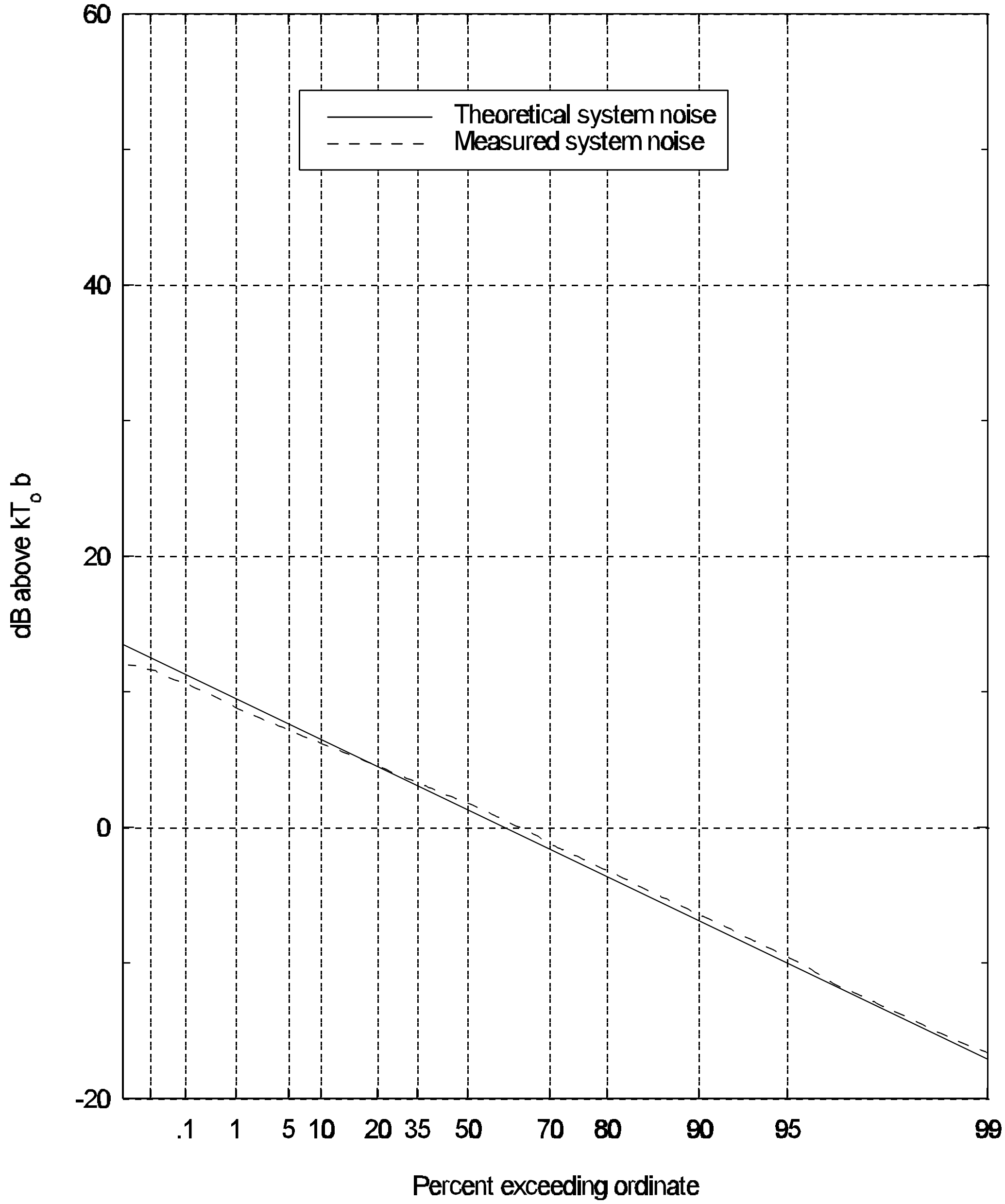

Figure 2.4 APD of receiver noise power.

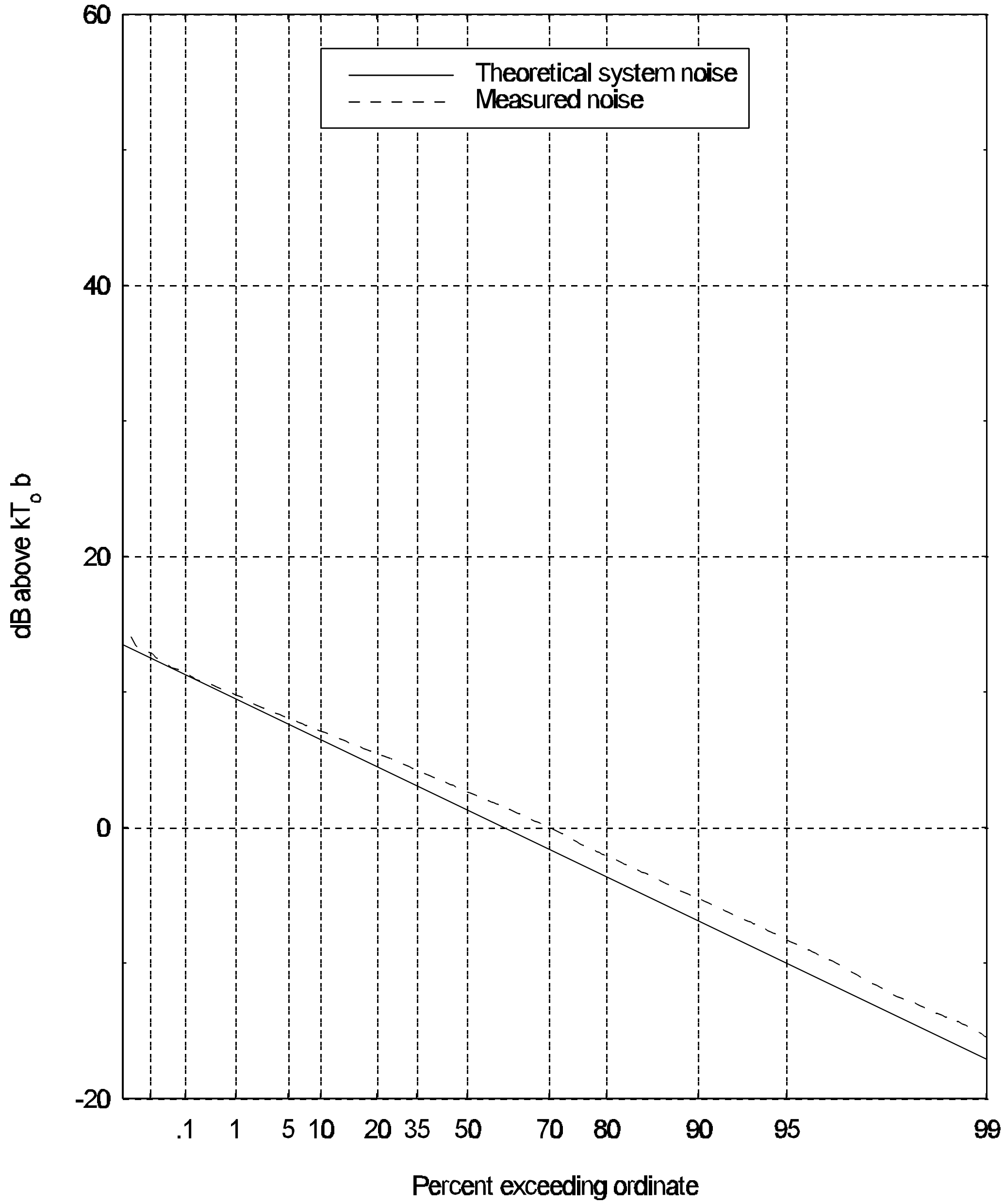

Figure 2.5 APD of environmental noise in a quiet canyon with power inverter on.

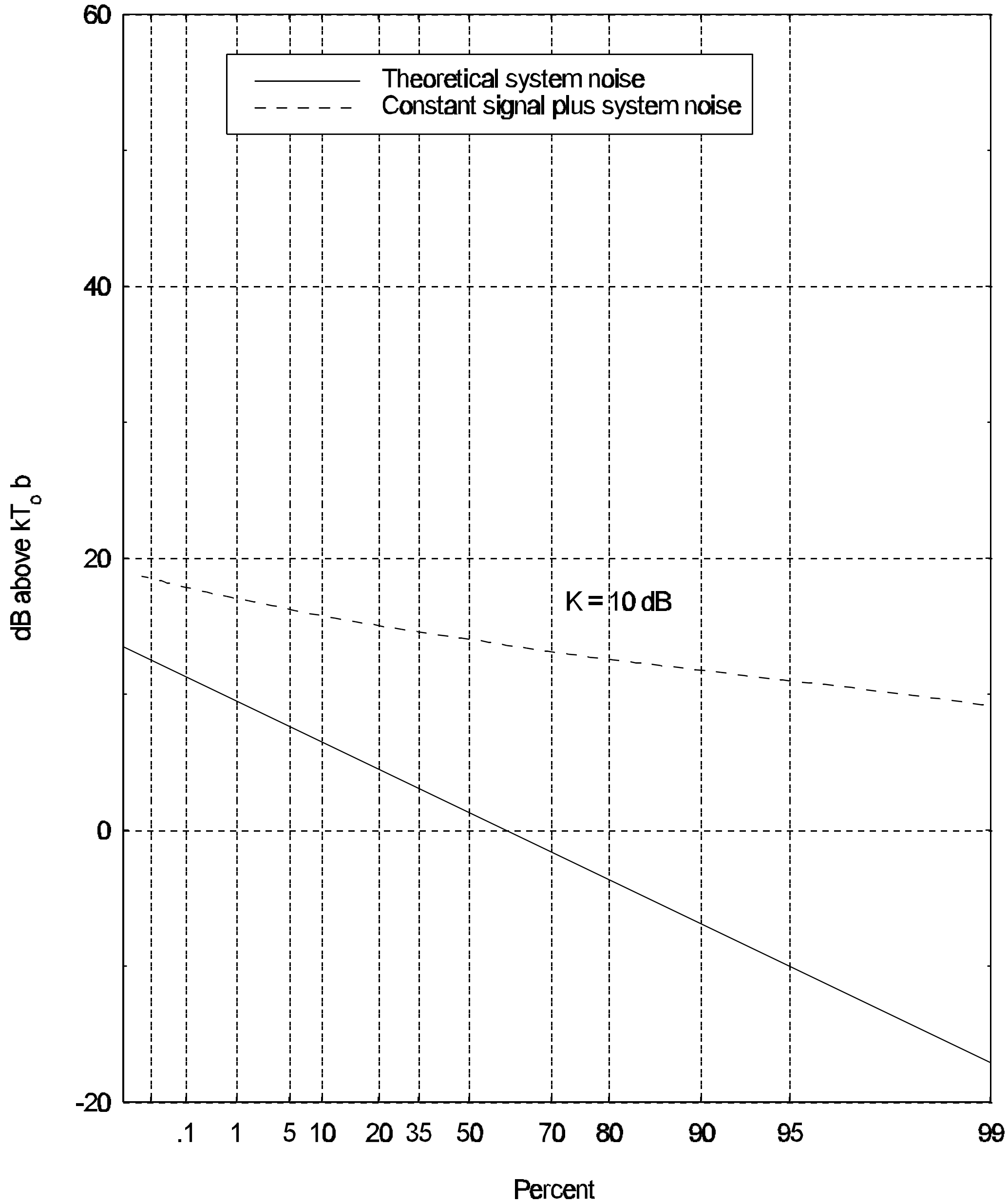

Figure 2.6 APD of a continuous wave signal with a 10-dB signal-to-noise ratio.